JOURNAL OF CATALYSIS 19, 216–226 (1970)

Apparent Activation Energies on Catalysts with Heterogeneous Surfaces

III. Atomically-Flat Surfaces on Body and Face-Centered Cubic Lattices

J. BAGG

Department of Industrial Science, University of Melbourne, Parkville, Victoria 3052, Australia

Received February 17, 1970

The heterogeneity of a catalyst surface has been estimated using hard sphere models. The number of sites of different free bond number was calculated for atomically-flat surfaces on body or face-centered cubic lattices. By substituting this theoretical heterogeneity into the equations derived previously the apparent activation energy and pre-exponential factor for simple first or zero-order reactions catalyzed by a single (*hkl*) plane or polycrystalline surfaces were found.

The model predicts that, despite the heterogeneity of the surface, the apparent rate constant will still appear to obey the Arrhenius equation. The apparent activation energy derived from this equation will, however, be very sensitive to the range of temperature used in its determination.

The activation energy for a first-order reaction will be independent of surface orientation. For a zero-order reaction, depending upon some assumptions, the activation energy for low-index planes is different from that for high-index planes or polycrystalline surfaces.

If the true activation energy and pre-exponential factor on individual types of site show the compensation effect, then a series of catalysts of different orientation or composition will also show compensation between apparent activation energy and pre-exponential factor. It is not necessary to postulate some special site distribution to obtain this result.

INTRODUCTION

The importance of the crystallographic orientation and structure of surfaces in catalytic theory is shown by the extensive discussions of the "geometric factor" (*1*) and by Balandin's theory of multiplets (*2*). The majority of catalysts of practical importance are polycrystalline and expose many crystal planes to the reactants. If these planes differ in catalytic activity then the apparent activation energy derived from the temperature-dependence of the overall rate will be a function of the area, activation energy and pre-exponential factor for each plane. Without some knowledge of the heterogeneity, the apparent activation energy is of limited value in comparing catalysts and catalytic reactions.

In Part I (*3*), equations were derived which related the apparent activation energy to any postulated type of heterogeneity. These equations would allow some progress to be made in the interpretation of activation energies if some estimate could be made of the heterogeneity due to crystal orientation. In recent years, models of surfaces have been constructed from hard spheres to aid the interpretation of results from field emission, adsorption and catalysis (*4–7*). The field ion patterns found by Müller provide evidence that, in some cases, these models are useful in simulating real surfaces (*6*). Using the hard sphere model, Nicholas has made extensive calculations of the number and type of bonds broken at the surface of a variety

of crystal lattices (*7–9*). As shown below, these calculations may also be applied to determine the number and type of adsorption site and thus the heterogeneity of crystal surfaces.

There are limitations to be considered in applying the model, for example, the catalyst surface may rearrange during the reaction. When silver is heated in oxygen visible facets are formed indicating a massive rearrangement (*10*).

The adsorption of oxygen by nickel appears to produce a crystal structure with different crystal parameters to the bulk (*11*). Even in the absence of adsorption there is some evidence of small changes in lattice parameter at the surface (*12*).

Another factor which must not be overlooked is the presence of defects such as dislocations and stacking faults which intersect the surface causing deviation from the idealized surface. It is possible, however, to make models which contain these defects and so to improve the approximation to real surfaces (*13*).

In view of the author, despite the above limitations, ball models seem valuable in simulating real surfaces and allowing semiquantitative conclusions to be drawn about adsorption and catalytic behavior. In this paper the number and types of sites on surfaces formed by the intersection of (*hkl*) planes with body-centered (BCC) or face-centered (FCC) cubic lattices, the most common structures of metal catalysts, have been calculated. By making various sets of assumptions about the activation energy and pre-exponential factors on individual sites the apparent activation energies for these planes were obtained.

Derivation

(i) Adsorption sites on (*hkl*) surfaces. If an infinite ideal crystal is imagined to be divided into two parts by a plane with Miller indices (*hkl*) the two new surfaces may be described as atomically-flat surfaces with indices (*hkl*) and ($\bar{h}\bar{k}\bar{l}$). Such a semi-infinite crystal with an atomically-flat surface is one in which all possible atomic positions are occupied one side of, and possibly on, the dividing plane but none are occupied on the other. If an interatomic bond is represented by a line segment terminated at each end by atoms then some of these bonds must be broken in the creation of the surface.

Atoms in the bulk of the crystal have a nearest-neighbor coordination of Z, where $Z = 8$ or 12 for BCC and FCC lattices, respectively, so that a surface atom will be any atom with less than Z nearest neighbors. Nicholas has given simple equations for the density (number of atoms/unit surface cell) of atoms with exactly $1, 2, 3 \ldots Y$ of the nearest-neighbor bonds broken (*7*). It has been postulated that directed orbitals can emerge at catalyst surfaces (*14, 15*) and that, on metals, the metal–adsorbate bond is essentially similar to the metal–metal bond (*14*). If the nearest-neighbor vectors are identified with directed orbitals then the number and location of broken bonds in the ball model define the number and type of adsorption site.

The configuration of catalyst atoms that constitute a site will depend upon the size, shape, and electronic structure of the adsorbed species. The reacting species will be assumed to be located within a sphere whose diameter is not greater than that of the underlying catalyst atoms. The reactive species are further assumed to be adsorbed in such a way that the imaginery spheres take up the same positions that catalyst atoms would occupy in adding one complete surface layer to the crystal. Depending upon the site, therefore, an adsorbed species will be bound by $1, 2, 3 \ldots Y$ bonds to the catalyst, where $Y = 4$ or 6 for BCC or FCC, respectively. On this basis then,

$$N_a(j, hkl) = N_s(j, hkl), \qquad (1)$$

$N_a(j, hkl)$ = number of species bound by j bonds to catalyst atoms/unit surface cell, $N_s(j, hkl)$ = number of sites with j free bonds/unit surface cell. An atomically-flat surface can be constructed from a unit surface cell repeated in two dimensions and the area of this cell, $A_u(hkl)$, can be calculated from the Miller indices and three-dimensional cell constants (*7*).

Consideration of the model shows that the bonds between adsorbed species and

catalyst atoms on an (hkl) surface are identical in number and geometry with the broken bonds on an $(\bar{h}\bar{k}\bar{l})$ surface, i.e.,

$$N_s(j, hkl) = N_c(j, \bar{h}\bar{k}\bar{l}),$$

By symmetry,

$$= N_c(j, hkl), \qquad (2)$$

$N_c(j, hkl)$ = number of catalyst atoms with exactly j broken bonds/unit surface cell.

The equations of Nicholas are concerned with the coordination of the catalyst atoms and give $N_c(j, hkl)$ but Eq. (2) allows these values to be used directly to give $N_s(j, hkl)$,

Catalyst atoms with the same number of nearest-neighbor bonds can differ with respect to the geometrical arrangement of their nearest neighbors. For example, on BCC surfaces there are two possible arrangements of neighbors around atoms with four broken bonds. It follows that there will be also two types of site differing only in the orientation of the four free bonds to the surface. On the simple hypothesis used in this derivation only the number of free bonds should govern adsorption and so all the sites with the same bond number are considered equivalent. The expressions for $N_s(j, hkl)$ on BCC surfaces are given in Table 1; the expressions for FCC are

TABLE 1

$N_s(j, hkl)$ FOR ANY (hkl) PLANE ON A BCC CRYSTAL $(h \geqslant k \geqslant l \geqslant 0)$

Free bond no.	Region A $(h - k - l \geqslant 0)$	Region B $(-h + k + l \geqslant 0)$
1	$2l$	$2l$
2	$2(k - l)$	$2(k - l)$
3	$2l$	$2(h - k)$
4	$h - k - l$	$-h + k + l$

more complicated and may be obtained from the original reference (9).

(ii) General expressions for apparent activation energy and pre-exponential factor. Equations (17a), (17b), (18a), (18b) from Part I are rewritten using the following symbols (3):

r_i = number of replicate measurements of $\ln k_{app}$ at reaction temperature T_i°K.

δ_i^2 = error variance of replicate measurements of $\ln k_{app}$ at T_i.

n = number of reaction temperatures used in determination;

$i = 1, 2, 3 \ldots n.$

$$x_i = 1/T_i; \; Sxx = \sum^{n} r_i(x_i - \bar{x})^2;$$

$$\bar{x} = \frac{\Sigma^n r_i x_i}{\Sigma^n r_i}; \; p = 0 \text{ or } 1$$

$$P_j = \frac{k_b t_j}{h} \exp(S_j/R)$$

k_b, h = Boltzmann and Plank constants,

S_j = entropy term [defined in Part I (3)] for a j-site,

t_j = transmission coefficient of the activated complex on a j-site.

The differences between the apparent activation energy E_a, and pre-exponential factor, A, and the activation energy, E_1, and pre-exponential factor, P_1, on sites of single free bond $(j = 1)$ are given by:

$$E_a - E_1 = \Delta E_C \pm \Delta E_E; \; \ln A - \ln P_1 = \Delta \ln A_C \pm \Delta \ln A_E$$

where ΔE_C, $\Delta \ln A_C$ are attributable to curvature and ΔE_E, $\Delta \ln A_E$, are attributable to experimental error (3).

$$\Delta E_C = \frac{R}{Sxx}\left\{p \sum^{n} r_i \ln x_i(x_i - \bar{x}) - \sum^{n} r_i \ln(1 + C(x_i))(x_i - \bar{x})\right\} + (E_m - E_1), \qquad (3)$$

$$\Delta \ln A_C = \ln Q + (\Delta E_C/R)\bar{x} + \frac{\Sigma^n r_i \ln(1 + C(x_i))}{\Sigma^n r_i} - \frac{p \, \Sigma^n r_i \ln x_i}{\Sigma^n r_i}. \qquad (4)$$

Two types of surface will be considered. First, a surface exposing a single (hkl) plane, secondly, a polycrystalline surface exposing many atomically-flat (hkl) planes, each plane being of sufficient area that grain boundaries occupy only a negligible fraction of the surface. For a single orientation,

$$C(x_i) = \sum_{j=M+1}^{Y} \frac{N_s(j, hkl)P_j}{N_s(M, hkl)P_M} \times \exp\left[\frac{(-(E_j - E_M)x_i)}{R}\right],$$

$N_s(M, hkl)$ = number of sites/unit surface cell with the minimum free bond number, M, found on that particular (hkl) surface, i.e., $M \geq 1$. This form for $C(x_i)$ is necessary because not all (hkl) planes contain single bond sites.

E_j, E_M = enthalpy terms (defined in Part I) for j- and M-sites,

$$Q = \frac{N_s(M, hkl)P_M}{A_u(hkl)P_1}$$

For a polycrystalline surface,

$$C(x_i) = \sum_{j=M+1}^{Y} \frac{g_s(j)P_j}{g_s(M)P_M} \times \exp\left[\frac{-(E_j - E_M)x_i}{R}\right]$$

$$g_s(j) = \sum_h \sum_k \sum_l \frac{w_{hkl}N_s(j, hkl)}{A_u(hkl)}$$

w_{hkl} = area of (hkl) surface/total polycrystalline area.

$$Q = \frac{g_s(M)P_M}{P_1}$$

The equations presented for ΔE_E and $\Delta \ln A_E$ are more general than in Part I because constant error variance δ_i^2, is not assumed.

$$\Delta E_E = \frac{Rt[\Sigma^n r_i(x_i - \bar{x})^2\delta_i^2]^{1/2}}{Sxx}, \quad (5)$$

$$\Delta \ln A_E = \frac{t[\Sigma^n r_i(Sxx - (\Sigma^n r_i x_i)^2 (x_i - \bar{x}))^2\delta_i^2]^{1/2}}{Sxx\Sigma r_i}, \quad (6)$$

$t = 1.96$ for 95% confidence limits (*16*).

Excellent approximations for ΔE_C and $\Delta \ln A_C$ which reduce arithmetical labor were possible in the case of dual-site catalysts and may also be used for the more complex surfaces described here (*17*). If the upper and lower temperatures used in the determination are T_2 and T_1 then with $x_h = \frac{1}{2}(x_1 + x_2)$,

$$\Delta \overset{*}{E}_C = \frac{pR}{x_h} + \frac{D(x_h) - E_M C(x_h)}{1 + C(x_h)} + (E_M - E_1) \quad (7)$$

$$\Delta \ln \overset{*}{A}_C = \ln Q + p - p \ln x_h + \ln(1 + C(x_h)) + \frac{x_h[D(x_h) - E_M C(x_h)]}{R(1 + C(x_h))}. \quad (8)$$

For a single orientation,

$$D(x_h) = \sum_{j=M+1}^{Y} \frac{E_j P_j N_s(j, hkl)}{E_M P_M N_s(M, hkl)} \times \exp\left[\frac{-(E_j - E_M)x_h}{R}\right].$$

For a polycrystalline surface,

$$D(x_h) = \sum_{j=M+1}^{Y} \frac{E_j P_j g_s(j)}{E_M P_M g_s(M)} \times \exp\left[\frac{-(E_j - E_M)x_h}{R}\right].$$

(iii) Assumptions concerning reactions. Equations (3–8) can be applied to all the reactions that fall within the restrictions laid down in Part I (*3*). However, to minimize assumptions about enthalpies and entropies of activation and adsorption further restrictions are applied in this paper. Firstly, the rate-determining step is assumed monomolecular to avoid the complication of reaction between two adjacent species on different types of site. Secondly, the assumption that the activated complex is the same on all types of site is extended to mean that the enthalpy of the activated complex, $H^{\#}$ (θ), is the same on all sites. The enthalpy of activation is, under these circumstances, governed by the heat of adsorption of the reacting species (*18*). For first-order reactions this assumption leads to a simple result; from Eq. (8) in Part I (*3*),

$$E_j = \Delta H_{12}^0(0, j) + \overline{\Delta H}_{12}^0(0, j)$$
$$= (H^\ddagger(0) - H_a(0)) + (H_a(0) - H_g)$$
$$= H^\ddagger(0) - H_g$$

where $H_a(0)$ = partial molar enthalpy of the adsorbed species at low coverage, H_g = molar enthalpy in the gas phase.

The activation energy, E_j, is, therefore, independent of the type of site and the surface will appear to be homogeneous. The expressions for ΔE_C and $\Delta \ln A_C$ are,

$$\Delta E_C = \frac{R\Sigma^n r_i \ln x_i (x_i - \bar{x})}{Sxx},$$

$$\Delta \ln A_C = \ln(N_T(hkl)/A_u(hkl)) + (\Delta E_C/R)\bar{x} - \frac{\Sigma^n r_i \ln x_i}{\Sigma^n r_i}, \quad (9)$$

$N_T(hkl)$ = total number of all types of site/unit surface cell. The first term in Eq. (9) only varies weakly with orientation so that the apparent activation energy and pre-exponential factor will, within experimental error, be the same on all (hkl) planes or polycrystalline surfaces.

At saturation coverage the enthalpy and entropy of activation will be governed by the heat and entropy of adsorption upon a given site and, consequently, by the type of site. The heat and entropy of adsorption should be greatest on sites with the maximum number of free bonds and least on sites with the minimum number of free bonds. The activation enthalpy and entropy will also vary in the same way; however, the exact nature of the dependency is not known and only empirical equations, $E_j = f(j)$, may be tested at present. From the above considerations, E_j and P_j must be related to each other and, from theoretical considerations of adsorption (*19*) and the large body of data on the compensation effect (*20, 21*), the following relationship appears to be generally applicable,

$$\ln P_j = \alpha + \beta E_j. \quad (10)$$

Results

Calculations for the apparent activation energy at saturation coverage were made using the following equations for E_j chosen to give linear, concave, and convex graphs (shown in Fig. 1),

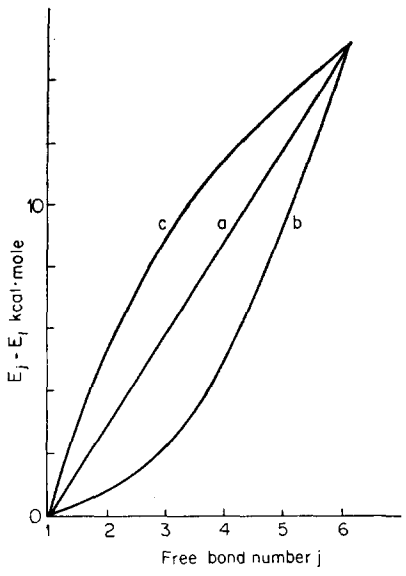

FIG. 1. $(E_j - E_1)$ vs j on FCC surfaces using (a) Eq. (11); (b) Eq. (12); and (c) Eq. (13) for $f(j)$.

$$E_j = E_1 + ([j - 1)/(Y - 1)]^2 \Delta E_{1Y}, \quad (11)$$

$$E_j = E_1 + [(j - 1)/(Y - 1)]\Delta E_{1Y}, \quad (12)$$

$$E_j = E_1 + [\log j/\log Y]\Delta E_{1Y}, \quad (13)$$

$$\Delta E_{1Y} = E_Y - E_1.$$

ΔE_{14}, ΔE_{16} were set equal to 10 and 15 kcal/mole, respectively, because these values lead to variations in apparent activation energies similar to some observed in practice (*18*).

The value of P_j/P_M for each value of E_j was calculated from Eq. (10) with β varied from 0 (no compensation) to 6×10^{-3}.

Measurements of log k_{app} were considered in ranges of 100° at reaction temperatures from 323 to 823°K. The number of reaction temperatures within the range were 4, 6, 11 spaced as follows,

n = 4, 323, 363, 403, 423;

n = 6, 323, 343, 363, 383, 403, 423;

n = 11, 323, 333, 343, 353, 363, 373, 383, 393, 403, 413, 423.

Values of $N_s(j, hkl)$ and $A_u(hkl)$ used in the calculations are given in Table 2 with an assumed catalyst atom radius of 1.35 Å, typical of many metallic catalysts. A stereographic plot of the normals to the

TABLE 2
$N_s(j, hkl)$ AND AREA OF UNIT SURFACE CELL FOR SURFACES ON BCC AND FCC CRYSTALS

(hkl)	Free bond no. j 1	2	3	4	$A_u(hkl)$ (Å²)
BCC surfaces					
(100)	0	0	0	1	9.72
(110)	0	1	0	0	6.87
(111)	2	0	0	1	16.84
(210)	0	2	0	1	21.73
(221)	2	2	0	1	29.16
(311)	2	0	2	1	32.24
(321)	1	1	1	0	18.18
(432)	4	2	2	1	44.54
(721)	1	1	1	2	35.71
(851)	1	4	1	1	46.11

FCC surfaces	1	2	3	4	5	6	
(100)	0	0	0	1	0	0	7.29
(110)	1	0	0	0	1	0	10.31
(111)	0	0	1	0	0	0	6.31
(210)	1	0	1	0	0	1	16.20
(221)	1	0	2	0	1	0	21.87
(311)	0	1	0	0	1	0	12.20
(321)	1	1	1	1	0	1	27.28
(432)	1	1	3	1	0	1	39.26
(721)	1	2	1	2	2	1	53.57
(851)	4	2	1	2	1	3	69.16

surfaces in Table 2 is shown in Fig. 2. Surfaces exposing a single plane are not commonly encountered so that calculations were also made for an "average surface," i.e., the surface of a polycrystalline aggregate in which grains are of random orientation. Such a surface may be approximated by the surface of a large hemisphere and

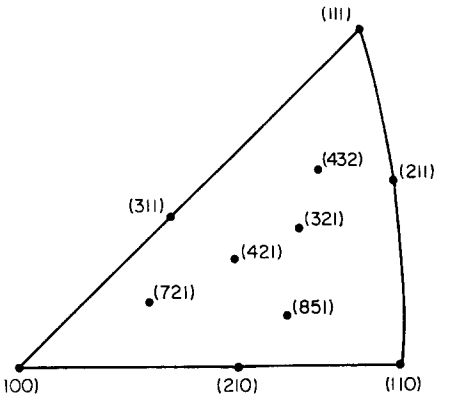

FIG. 2. Stereographic projection of the normals to the surfaces shown in Table 2.

the site density, $g_s(j)$, taken from the calculations of Nicholas (8), for this surface is given in Table 3.

In general, the graph of log k_{app} vs $1/T_i$ is not linear for reactions over a heterogeneous surface (3). A comparison of the degree of curvature predicted for the model with that observed using practical catalysts is a useful test of the model. Using Eqs. (19) from Part I (3) and (4) from Part II (17), the percentage confidence limits ($\pm$CL%), required of an individual measurement of k_{app} in order to detect curvature were calculated. If these confidence limits are greater than the experimental accuracy then curvature will be detected.

(a) Dependence of apparent activation energy upon the number of reaction temperatures. In Table 4, ΔE_C and $\Delta \log A_C$ are shown for different values of n with an equal number of replicate measurements at each reaction temperature, $r_i = r$ for all i.

TABLE 3
$g_s(j)$, (no. of j-sites/cm² $\times 10^{-16}$) ON AN "AVERAGE SURFACE"

	Free bond no. j 1	2	3	4	5	6
BCC						
$g_s(j)$	0.2303		0.2733	0.1539		0.1656
FCC						
	1	2	3	4	5	6
$g_s(j)$	0.2733	0.2270	0.3117	0.1943	0.2405	0.1689

TABLE 4

A COMPARISON OF $\Delta\overset{*}{E}_C$(kcal/mole), $\Delta \log \overset{*}{A}_C$ WITH ΔE_C, $\Delta \log A_C$ DERIVED FROM DIFFERENT NUMBERS, n, OF REACTION TEMPERATURES

BCC lattice: temp range, 432–523°K; $\beta = 1.2 \times 10^{-3}$.

No. of measurements used for ΔE_C	4		6		11			
(hkl)	ΔE_C	$\Delta \log A_C$	ΔE_C	$\Delta \log A_C$	ΔE_C	$\Delta \log A_C$	$\Delta\overset{*}{E}_C$	$\Delta \log \overset{*}{A}_C$
(100)	10.93	23.33	10.93	23.33	10.93	23.33	10.93	23.33
(210)	7.79	21.80	7.81	21.81	7.82	21.81	7.81	21.79
(311)	7.34	21.62	7.37	21.63	7.40	21.64	7.43	21.64
(432)	5.91	20.91	5.93	20.92	5.95	20.92	5.93	20.90
(721)	8.48	22.17	8.50	22.18	8.53	22.18	8.57	22.19

These terms were almost independent of n and calculations over a wider range showed similar independence for all ranges likely in practice. Table 4 also shows that $\Delta\overset{*}{E}_C$, $\Delta \log \overset{*}{A}_C$ are excellent approximations to ΔE_C, ΔA_C; over a wide range of conditions the difference between $\Delta\overset{*}{E}_C$ and ΔE_C will rarely exceed 0.05 ΔE_C. Except for the most accurate work, E_a is, therefore, most conveniently given by $E_1 + \Delta\overset{*}{E}_C \pm \Delta E_E$.

(b) Dependence of curvature upon orientation, temperature and β. Values of ±CL% are given in Table 5 and show that, except when $\beta = 1.2 \times 10^{-3}$, the curvature will not be detectable under normal experimental conditions. The condition $n = 11$ used in the construction of Table 5 is rather stringent because apparent activation energies are more often obtained from 4 or 6 reaction temperatures. Under the less stringent conditions even with $\beta = 1.2 \times 10^{-3}$ curvature will not be detected.

(c) Dependence of apparent activation energy upon E_j, β, and temperature range. Values of ΔE_C for (hkl) and "average sur-

TABLE 5

THE EXPERIMENTAL ACCURACY OF k_{app} (±CL %) REQUIRED TO DETECT CURVATURE IN THE GRAPH $\log k_{app}$ VS $1/T$ FOR REACTIONS ON FCC SURFACES

Eq. used for $f(j)$:	$\beta = 0.4 \times 10^{-3}$			$\beta = 1.2 \times 10^{-3}$			$\beta = 2.0 \times 10^{-3}$		
(hkl)	(11)	(12)	(13)	(11)	(12)	(13)	(11)	(12)	(13)
				Temp range 323–423°K					
(100)	0.32	0.32	0.32	0.32	0.32	0.32	0.32	0.32	0.32
(210)	0.60	0.39	0.38	8.07	10.74	13.61	0.39	0.55	0.88
(311)	0.33	0.33	0.34	7.47	7.47	6.17	0.53	0.53	0.65
(432)	0.78	0.77	0.42	4.37	7.60	12.74	0.70	1.50	2.19
(721)	0.56	0.87	0.49	7.19	10.04	14.14	1.79	2.02	1.39
Av. surf.	0.59	0.62	0.39	6.31	9.55	13.79	1.45	1.81	1.50
				Temp range 623–723°K					
(100)	0.10	0.10	0.10	0.10	0.10	0.10	0.10	0.10	0.10
(210)	0.20	0.24	0.39	0.14	0.19	0.23	0.10	0.10	0.10
(311)	0.27	0.27	0.29	0.17	0.17	0.19	0.10	0.10	0.10
(432)	0.22	0.50	0.72	0.27	0.43	0.41	0.10	0.10	0.11
(721)	0.32	0.51	0.75	0.45	0.37	0.25	0.10	0.12	0.13
Av. surf.	0.26	0.45	0.55	0.40	0.37	0.28	0.10	0.11	0.12

TABLE 6
ΔE_C(kcal/mole) FOR FCC SURFACES ($n = 11$, $r_i = 1$ for all i)

Eq. used for $f(j)$:	$\beta = 0.4 \times 10^{-3}$			$\beta = 1.2 \times 10^{-3}$			$\beta = 2.0 \times 10^{-3}$		
(hkl)	(11) ΔE_C	(12) ΔE_C	(13) ΔE_C	(11) ΔE_C	(12) ΔE_C	(13) ΔE_C	(11) ΔE_C	(12) ΔE_C	(13) ΔE_C
				Temp range 423–523°K					
(100)	6.33	9.93	12.53	6.33	9.93	12.53	6.33	9.93	12.53
(110)	0.95	0.93	0.94	8.20	10.52	12.02	10.53	12.93	14.43
(111)	3.33	6.93	10.13	3.33	6.93	10.13	3.33	6.93	10.13
(210)	1.33	1.04	0.96	12.02	12.19	12.61	15.93	15.93	15.91
(221)	1.63	1.15	0.98	6.41	9.04	11.13	10.51	12.88	14.27
(311)	1.56	3.96	6.78	8.24	10.64	12.25	10.53	12.93	14.43
(321)	1.48	1.40	1.08	10.27	10.92	11.90	15.93	15.91	15.76
(432)	1.80	1.57	1.11	9.12	10.08	11.45	15.93	15.90	15.71
(721)	1.55	1.68	1.20	9.59	11.06	12.44	15.86	15.56	15.26
(851)	1.22	1.16	1.00	10.98	11.57	12.32	15.92	15.85	15.72
Av surf.	1.49	1.36	1.06	9.42	10.71	12.01	15.88	15.66	15.40
				Temp range 623–723°K					
(100)	6.73	10.33	12.93	6.73	10.33	12.93	6.73	10.33	12.93
(110)	1.66	1.52	1.46	10.80	13.28	14.79	10.93	13.33	14.83
(111)	3.73	7.33	10.53	3.73	7.33	10.53	3.73	7.33	10.53
(210)	2.11	2.06	1.77	16.27	16.15	15.91	16.33	16.33	16.33
(221)	2.60	2.64	2.13	10.28	12.56	13.84	10.93	13.33	14.79
(311)	2.31	4.71	7.62	10.77	13.17	14.59	10.93	13.33	14.83
(321)	2.34	2.81	2.52	16.11	15.74	15.31	16.33	16.33	16.28
(432)	2.71	3.44	3.02	16.02	15.49	14.82	16.33	16.33	16.27
(721)	2.61	3.42	3.26	15.23	14.75	14.86	16.32	16.19	15.91
(851)	1.99	2.15	1.95	16.04	15.76	15.58	16.33	16.31	16.23
Av. surf.	2.42	2.82	2.49	15.48	15.00	14.94	16.32	16.23	16.02

faces" on FCC lattices are given in Table 6. The magnitude of ΔE_C is dependent upon the choice of $f(j)$ but the general pattern of its variation with orientation, temperature and β is not. This independence is illustrated in Fig. 3 where the shape of the curve and the shift with temperature is very similar for all three functions tested. Some general conclusions can, therefore, be drawn from the ball model without detailed knowledge of $f(j)$, provided that it is not some unusual function.

The strong variation of ΔE_C with β is shown in Figs. 4 and 5. When $\beta \leqslant 0.4 \times 10^{-3}$, ΔE_C is greatest on planes of low indices, BCC surfaces (100), (111), (210) and FCC surfaces (100), (111), but is small and almost independent of orientation on all other surfaces. When $\beta \geqslant 1.2 \times 10^{-3}$, ΔE_C is smallest on planes of low indices, BCC surface (110) and FCC surfaces (100), (111), and has larger values on all other surfaces. The compensation effect is weak for $\beta \leqslant 0.4 \times 10^{-3}$ and strong when $\beta \geqslant 1.2 \times 10^{-3}$.

In Figs. 3, 4, and 5 the limits $\pm\Delta E_E$ are marked for an experimental accuracy of $\pm 5\%$ in k_{app}, and show that the orientation dependence will be masked by experimental error in some cases.

The apparent activation energy is dependent upon the temperature range used for its determination. The dependence is strong for some orientations, e.g. (210) surface on FCC, and weak for others, e.g. (100) surface on FCC. Of more interest, because most catalysts are polycrystalline, is the effect of temperature for "an average surface." The following example indicates a variation that might occur in practice:

$E_1 = 10$ kcal/mole, $\Delta E_{16} = 15$ kcal/mole, $\beta = 1.2 \times 10^{-3}$,

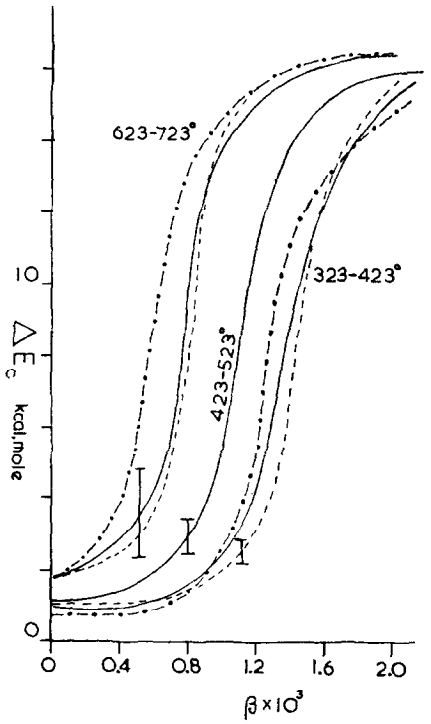

FIG. 3. ΔE_C vs β at various temperatures for an "average surface" on an FCC lattice: (vertical bars) the limits $\Delta E_C + \Delta E_E$ and $\Delta E_C - \Delta E_E$; (– – –) $f(j)$ given by Eq. (12); (——) Eq. (11); (· —) Eq. (13).

$n = 11$, experimental accuracy $\pm 5\%$, $f(j)$ from Eq. (12),

Temp. (°K)	E_a (kcal/mole)
323–423	13.4–12.6
423–523	21.2–20.2
723–823	26.4–24.0

DISCUSSION

The only experimental data for a zero-order reaction carried out over surfaces of known orientation appear to be those for the decomposition of formic acid vapor over silver (*18*, *22*). Even this system does not meet exactly the conditions of the model because adsorption data indicate that there is not a one-to-one correspondence between sites and formic acid molecules (*23*). The observed apparent activation energies were in the order, polycrystalline > (100) > (111) and there was strong compensation with $\beta = 1.1 \times 10^{-3}$. Figures 3 and 5 show that for $\beta \geqslant 1.2 \times 10^{-3}$ the model predicts the same order. No significant curvature was detected in the graphs of log k_{app} vs $1/T$ as anticipated for the experimental accuracy used.

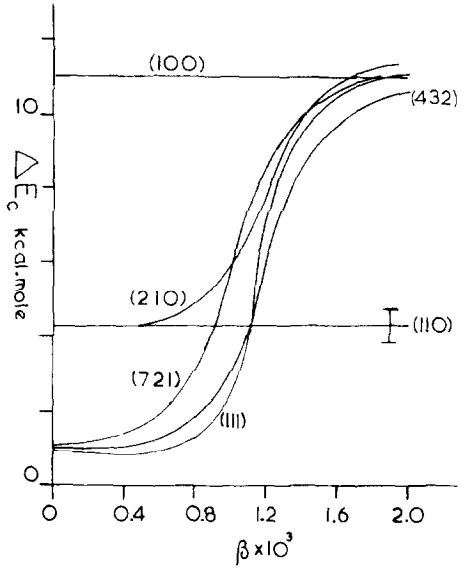

FIG. 4. ΔE_C vs β for different orientation on a BCC surface with temperature range 423–523°K.

Apart from the special case above, there

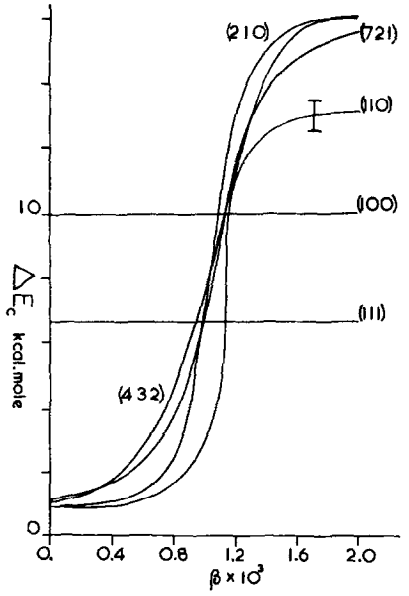

FIG. 5. ΔE_C vs β for different orientations on a FCC surface with temperature range 423–523°K.

are two generally observed features of catalytic reactions consistent with the model. First, the apparent activation energy does not, with the exception of some reactions on low index planes, appear to be very sensitive to surface orientation. Duplicate preparations of polycrystalline catalysts are unlikely to have the same surface structure yet the difference between their apparent activation energies usually falls within experimental error. The model shows that the activation energy for first-order reactions is independent of orientation and that for zero-order reactions differences due to orientation will often lead to only small effects masked by experimental error.

Secondly, in the majority of cases, apparent rate constants obey the Arrhenius equation without detectable curvature as predicted. One important conclusion to be drawn from the model is that, although the Arrhenius equation is obeyed, the apparent activation energy may be very sensitive to the temperature range. This effect should be borne in mind when comparing data not obtained under similar conditions.

Another feature common to many reactions is the compensation effect. By a suitable choice of conditions the model should be able to lead to this result from the basic assumption of compensation between true activation energy and pre-exponential factor, Eq. (10), on individual sites. There are two cases to be considered, first, surfaces of the same composition but different orientation and, secondly, surfaces of different composition and orientation. As an example of the second case the decomposition of formic acid vapor over a series of different polycrystalline metals may be cited (*24*). For the first case, Eq. (10) may be rewritten in terms of the compensation temperature, T_c,

$$B_1 \exp(-E_1/RT_c) = B_j \exp(-E_j/RT_c), \tag{14}$$

with $T_c = 1/R\beta$;

$\ln A$ and E_a may be related by using the fact that $\overset{*}{E}_a \pm \Delta E_E$ is a very good approximation to E_a, and then from Eqs. (7), (8), and (14),

$$\ln \overset{*}{A} = \ln \frac{(N_s(M, hkl)P_1)}{A_u(hkl)} - p \ln x_h - \frac{E_1 x_c}{R} + \ln(1 + C(x_h)) + \frac{\overset{*}{E}_a x_h}{R}.$$

The first term is almost independent of orientation and, for the same temperature range, a linear relationship between $\overset{*}{E}_a$ and $\ln \overset{*}{A}$ is obtained if $x_c = x_h$. Under these circumstances,

$$\ln \overset{*}{A} = \ln \left[\frac{N_s(M, hkl)P_1}{A_u(hkl)} \right] - p \ln x_h - \frac{E_1 x_c}{R} + \frac{\overset{*}{E}_a x_h}{R}. \tag{15}$$

The apparent activation energy and pre-exponential factor will be scattered around this line within limits $\pm\Delta E_E$ and $\pm\Delta \ln A_E$ and because of this scatter T_c and T_h can differ considerably before curvature becomes detectable.

This treatment can be extended readily to catalysts of different composition by postulating that Eq. (14) holds for all sites, irrespective of composition, i.e.,

$$B_1^A \exp(-E_1^A/RT_c) = B_1^B \exp(-E_1^B/RT_c) = B_j^X \exp(-E_j^X/RT_c),$$

where the superscript refers to the composition and the subscript to the type of site. The first term in Eq. (15) will be slightly modified but the slope of the line will still be x_h/R.

At present no theoretical justification can be given for the choice of T_c but it may be noted that several reactions have given experimental slopes close to the predicted slope (*17*).

The ball model is capable of extensions by calculations involving next-nearest as well as nearest neighbors in the definition of a site (*8*), by considering the size and shape of the adsorbed species when their diameter exceeds that of the catalyst atom defining a site, and by allowing for the intersection of defects with the surface (*13*). The chief limitation at present is the assignment of enthalpies and entropies appropriate to these surfaces.

References

1. Thomas, G. C., and Thomas, W. J., "Introduction to the Principles of Heterogeneous Catalysis," p. 299. Academic Press, London/New York, 1967.
2. Balandin, A. A., *in* "Catalysis and Chemical Kinetics" (A. A. Balandin *et al.*, eds.), Chap. 1. Academic Press, London/New York, 1964.
3. Bagg, J., *J. Catal.* **16,** 370 (1970).
4. Becker, J. A., *Advan. Catal. Relat. Subj.* **7,** 135 (1955).
5. Wortman, R., Gomer, R., and Lundy, R., *J. Chem. Phys.* **27,** 1099 (1957).
6. Müller, E. W., *Z. Phys.* **156,** 399 (1959).
7. Nicholas, J. F., "An Atlas of Models of Crystal Surfaces," Gordon and Breach, New York, 1965.
8. Nicholas, J. F., *J. Phys. Chem. Solids* **23,** 1007 (1962).
9. Mackenzie, J. E., Moore, A. J. W., and Nicholas, J. F., *J. Phys. Chem. Solids* **23,** 185 (1962).
10. Moore, A. J. W., *Acta Met.* **10,** 579 (1962).
11. Germer, L. H., and Macrae, A. U., *J. Chem. Phys.* **37,** 1382 (1962).
12. Germer, L. H., and Hartman, C. D., *J. Appl. Phys.* **31,** 2085 (1960).
13. Jaeger, H., and Sanders, J. V., *J. Res. Inst. Catal., Hokkaido Univ.* **16,** 287 (1968).
14. Dowden, D. A., and Wells, D., *Actes Int. Congr. Catal. 2nd, 1960* **2,** 1499 (1961).
15. Eley, D. D., *Discuss. Faraday Soc.* **8,** 34 (1950).
16. Acton, F. S. *in* "Analysis of Straight-Line Data," p. 23. Dover, New York, 1959.
17. Bagg, J., *J. Catal.* **16,** 377 (1970).
18. Jaeger, H., *J. Catal.* **9,** 237 (1967).
19. Everett, D. H., *Trans. Faraday Soc.* **46,** 957 (1950).
20. Kemball, C., *Pro. Roy. Soc., Ser. A* **217,** 376 (1953).
21. Bond, G. C., "Catalysis by Metals," p. 140. Academic Press, London/New York 1962.
22. Sosnovsky, H. M. C., *J. Chem. Phys.* **23,** 1486 (1955).
23. Tamura, K., *Trans. Faraday Soc.* **55,** 1191 (1959).
24. Ref. (*21*), p. 422.